Morphology Evolution of Three-Dimensional Scours Under Submerged Jets

Ke-ling Chen, Wang-ru Wei* and Jun Deng

State Key Laboratory of Hydraulics and Mountain River Engineering, Sichuan University, Chengdu, China

Through physical model tests, the three-dimensional morphological features and their scale changes with time were measured and comparatively analyzed during the scouring of a homogeneous granular bed surface using submerged oblique jets. The effects of various flow velocities and water cushion depths on the depth, length, and width of the scour hole were studied. At the early stage of scour formation, the morphological scales changed more dramatically, and the jet impact flow velocity had a more significant effect on the scour hole relative to the depth of the water cushion; for the final scales in all three directions of the scour, the scour depth developed at a more significant rate relative to the length and width of the scour. The correlation between the depth, length, and width of scour hole formation was achieved based on the time-domain variation pattern of scour hole scales. As the jet velocity increased and the depth of the water cushion decreased, the scour gradually developed from a wide-shallow morphology to a narrow-deep morphology; the impact of three-dimensional morphological features of the scour on hole depth gradually became obvious, appearing to inhibit the development of scour depth. The results of the present experimental tests offered an exploratory study of the effect of three-dimensional morphological features on the formation of jet scours, having constituted the basis for more rational analysis and evaluation of energy dissipation for the hydraulic operation in water conservancy projects.

Keywords: scour evolution, three-dimensional morphology, impingement jet, time domain process, hydraulic model

INTRODUCTION

Jet scours in river beds are a common hydraulic issue in the fields of geomorphology and hydraulic engineering applications (in **Figure 1**). Insufficient understanding of hydraulic scours and improper treatment may cause destructive actions, such as dam breaks and river bed erosion (Boniforti et al., 2015; Yao and Wu, 2020; Qian et al., 2021). Mason showed the effects of jet aeration and discharge conditions on the final two-dimensional scour and proposed a formula for the scour depth calculations (Manson, 1989). Based on a series of experimental tests, the two-dimensional scour geometry was depicted by Canepa and Hager (2003). Their experimental results described the primary definition to account for the effects of aerated jets on scour generation. Using two sine functions, the axial scour profile was determined with non-dimensional parameters. The jet scour involved a complex hydraulic phenomenon, from upstream impact to tailwater conditions. The laboratory experimental tests were an effective way to describe the scour process due to the complexity of the scour mechanism (Lenzi et al., 2002; Gaudio and Marion, 2003), and some estimation equations were proposed for the equilibrium scour depth with

FIGURE 1 | Field sampling of water scouring.

its temporal evolution (Meftah and Mossa, 2006; Liu et al., 2018; Wang et al., 2018; Wang et al., 2020). Considering the jet diffusion theory of an empirical nature, a methodology with grade control structures and steady flow conditions was proposed to overcome some limitations in the scour generation (Beltaos and Rajaratnam, 1973; Bormann and Julien, 1991; Li et al., 2017).

In recent years, many studies have focused on the problem of hydraulic scour evolution. Dey and Barbhuiya (2005) conducted jet scour experiments to determine the time variation and equilibrium of scour depths for uniform and non-uniform sediments. Pagliara et al. (2006) summarized the time-domain evolution process of the two-dimensional scour for different incident angles, jet shape, velocity, aeration, and tailwater conditions, concluding that the relative jet impingement intensity was the important factor in scour evolution. They first investigated the three-dimensional plunge pool scour, and the temporal evolution process of scour depth was described (Pagliara et al., 2016; Pagliara and Palermo, 2017; Pagliara et al., 2020). The temporal scour profile development for dry conditions was measured by laboratory experiments, and the simple logarithmic relationship was given between developing and developed scour holes (Canepa and Hager, 2003; Pagliara et al., 2008). These relative research studies emphasized that the developing scour phase was mainly affected by the turbulent features, and it was different to assess the scour generation without the dynamic process. A complex morphological scour compared to the two-dimensional scour was obtained experimentally. Many researchers investigated the flow structures in the equilibrium scour stage (Liu et al., 1998; Adduce and Rocca, 2006; Guan et al., 2014). Dey and Sarkar (2008) studied the flow structure variations with time in a scour hole. A simplified model was proposed for the scours at various typical instants, which inevitably introduced disturbance in the flow velocity fields (Hill and Younkin, 2006). Bombardelli et al. (2018) used the optical principle to study the temporal evolution of a jet with an incident angle under different downstream conditions, and they confirmed that the temporal evolution of the scour can be divided into developing and developed shapes. Therefore, it is necessary to study the scour evolution

of the three-dimensional morphology. Detailed experiments about three-dimensional morphological features on the formation of jet scours are needed for further understanding of the jet-solid interactions and predictions.

For the natural process of jet scouring, the scour hole has a typical three-dimensional morphology and a time-domain evolution process. In this study, the three-dimensional scour scales with time development were measured experimentally under different submerged jet and water cushion depth conditions. Detailed analysis of the relationships among the scour depth, length, and width was conducted to provide insight into the scour morphological features. Moreover, a comparison between the two-dimensional and three-dimensional scour holes was discussed to obtain the general difference on the scour evolution process.

TEST METHODS AND HYDRAULIC CONDITIONS

The model scour test was performed in a 1.50-m-long, 1.00-m-wide, 0.75-m-high glass water tank using a circulating water supply and return system. The test layout is shown in **Figure 2** and principally consists of a supply tank, a jet lead section, a scour area, and a backwater area. The test flow was measured using a triangular thin-walled measuring weir located downstream of the scour area. The approach jet was controlled by a rectangular nozzle section, where the nozzle thickness b = 3 cm, the nozzle length W = 6.7 cm, and the incident angle of the jet θ = 60°; the nozzle outlet was submerged approximately 3 cm below the free surface. The inflow water velocity was regulated in that order. The depth T of the water cushion above the scour bed surface was controlled at 0.42, 0.47, and 0.52 m. The bed scour material was made of granular crushed gravels with a density ρ_s of approximately 2.2 g/cm^3. The suitable granular sands were screened out, and almost uniform sands were used for the present experiment with an average particle size of d = 3.0 mm. For the hydraulic scour test study, as it involved the scour resistance characteristics of the sediment, the sediment Froude number Fr_d was used as the hydraulic parameter to evaluate the impact and effect of water flow,
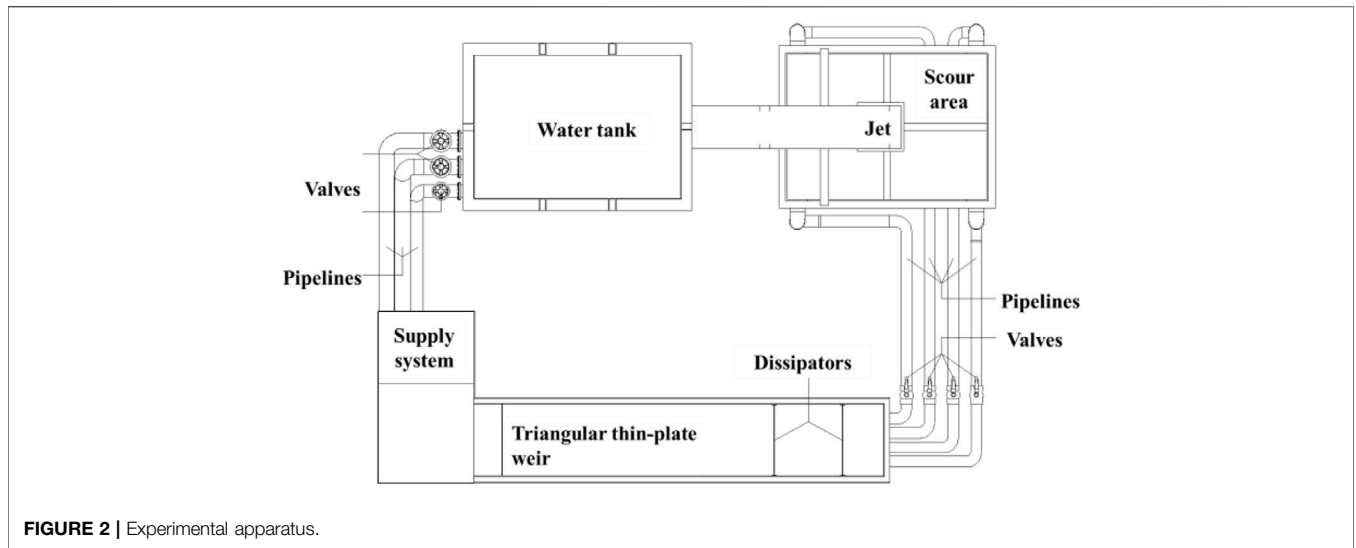
FIGURE 2 | Experimental apparatus.

TABLE 1 | Test programs.

No.	V (m/s)	Q (L/s)	Fr_d (-)	T (m)
1	1.0	2.0	5.3	0.42
2	1.3	2.6	6.9	0.42
3	1.5	3.0	8.0	0.42
4	1.8	3.6	9.6	0.42
5	2.2	4.4	11.7	0.42
6	1.0	2.0	5.3	0.47
7	1.3	2.6	6.9	0.47
8	1.5	3.0	8.0	0.47
9	1.8	3.6	9.6	0.47
10	2.2	4.4	11.7	0.47
11	1.0	2.0	5.3	0.52
12	1.3	2.6	6.9	0.52
13	1.5	3.0	8.0	0.52
14	1.8	3.6	9.6	0.52
15	2.2	4.4	11.7	0.52

FIGURE 3 | Definition scheme with notations.

defining $Fr_d = V/(g'd)^{0.5}$, where $g' = g\,[\rho_s\text{-}\rho]/\rho$ (Canepa and Hager, 2003); g represents the acceleration of gravity; and ρ_s and ρ denote the densities of sediment and water, respectively; the test conditions are shown in **Table 1**.

Since the start of the scour test, the deepest part of the scour, the side of the mound, and the farthest downstream position were observed and measured with a point gauge. The three-dimensional morphological data on the depth, width, and length of the scour hole were obtained every 5 min. The jet scour time was so determined that the rate of change in the size of the scour hole over five consecutive measurements was less than 0.5%. The three-dimensional morphological generalized characteristics of the jet scour are shown in **Figure 3**, with the difference in elevation between the deepest point and the bed surface as scour depth H, with the farthest longitudinal distance of the hole depth point from the downstream mound as the affected length of scour L, and with the farthest lateral distance from the lateral mound as the affected width of scour B. Upon final stabilization, the three-dimensional scales of the scour hole were H_u, L_u, and B_u, and the relative scales of the scour hole over time were defined as H/H_u, L/L_u, and B/B_u.
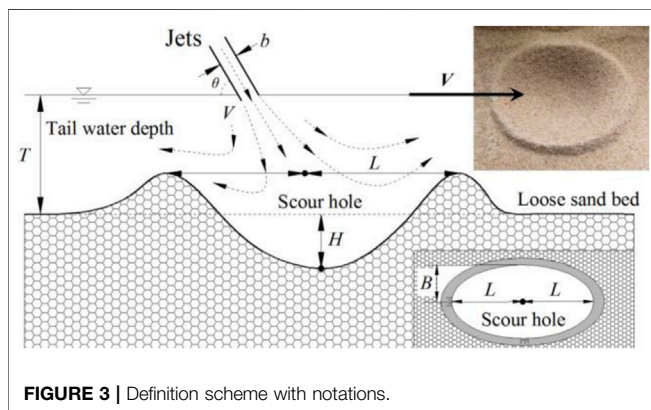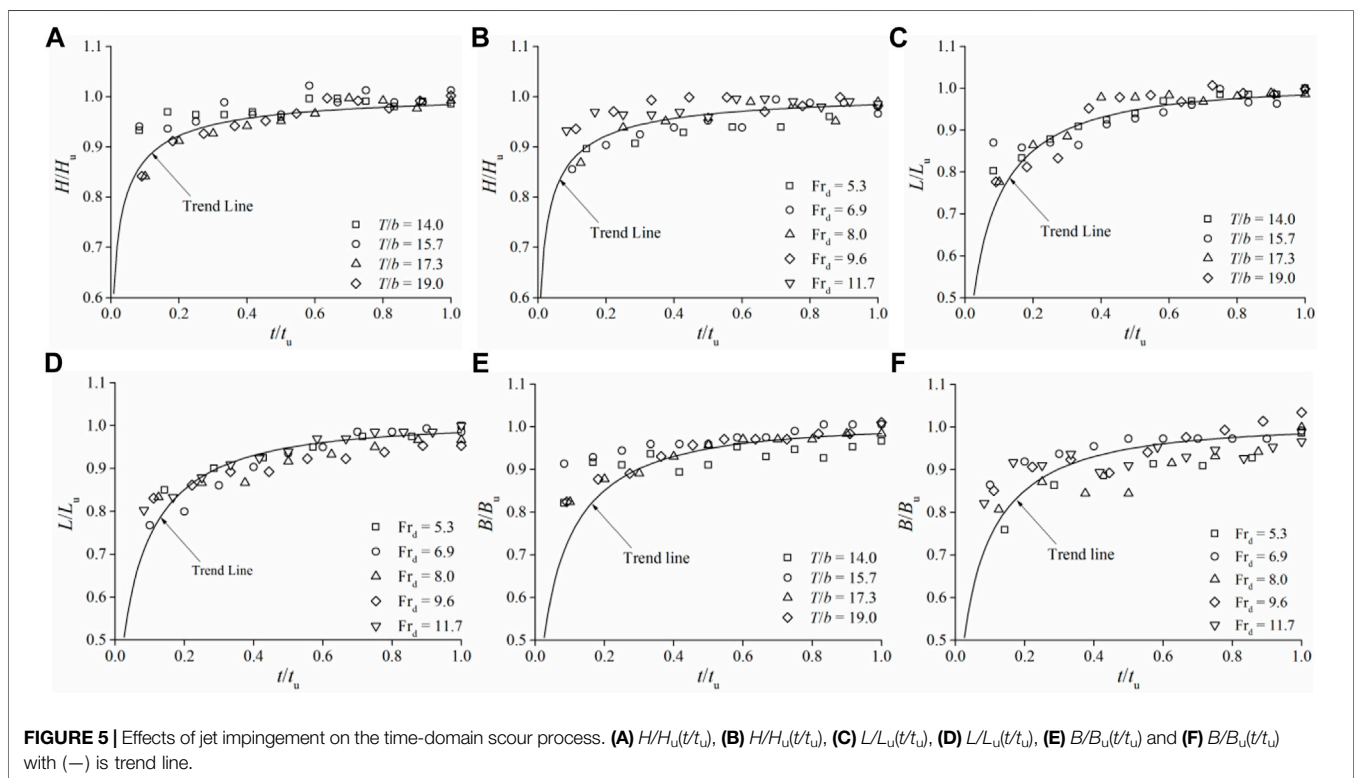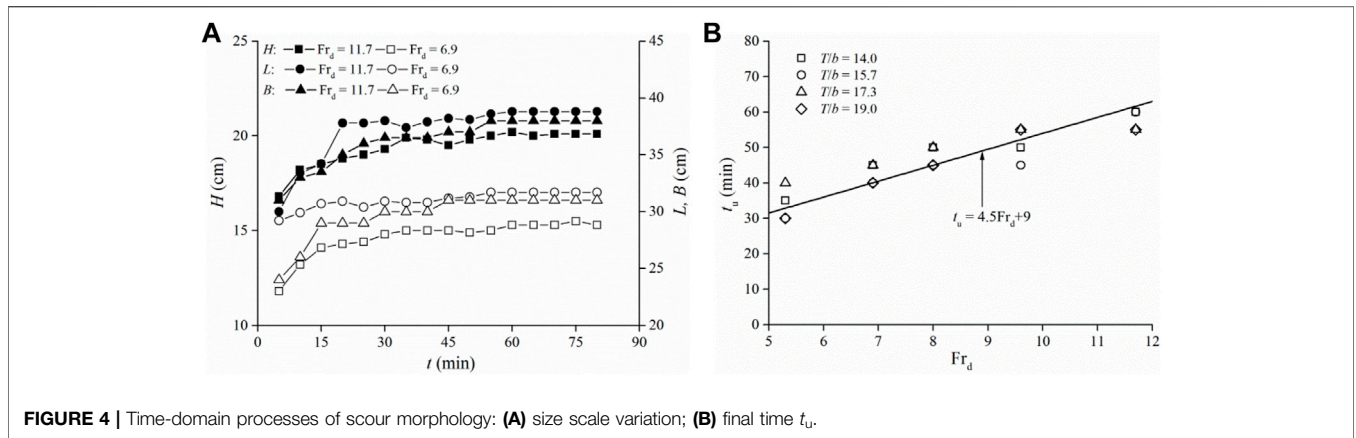
TIME-DOMAIN PROCESS ANALYSIS OF JET SCOURS

Figure 4A illustrates the typical course of variation in the depth, length, and width of the two sets of scour holes over time with water cushion depth $T = 0.42$ m, $Fr_d = 6.9$, and $Fr_d = 11.7$; since the onset of scouring ($T = 0$), the increase was significant in all three directions; as the scour continued to develop, the gradient of scale variation in all three directions diminished and gradually reached a stable final state; moreover, the three-dimensional scales were relatively consistent over time, and the depth, length, and width of the scour substantially reached a relatively stable state in the same period; the relative stabilization time for the scour process ranged from approximately 30 min to over 60 min. According to the test result of different flow rates and water cushion conditions, the final stabilization time t_u was less influenced by the depth of the water cushion for each condition and gradually increased with the

FIGURE 4 | Time-domain processes of scour morphology: **(A)** size scale variation; **(B)** final time t_u.

FIGURE 5 | Effects of jet impingement on the time-domain scour process. **(A)** $H/H_u(t/t_u)$, **(B)** $H/H_u(t/t_u)$, **(C)** $L/L_u(t/t_u)$, **(D)** $L/L_u(t/t_u)$, **(E)** $B/B_u(t/t_u)$ and **(F)** $B/B_u(t/t_u)$ with (—) is trend line.

increase in water flow Fr_d. As shown in **Figure 4B**, the variation approximately obeyed a linear relationship, provided by $t_u = 4.5Fr_d+9$. To further analyze the pattern of relative changes in the three-dimensional scale during the development of the scour, this fit equation was used to determine the scour time required for the relative stability of scour development under conditions where Fr_d and T are constant.

Figure 5 shows the relative scale variation of the scour depth, length, and width over time with reference to the relative stability time and three-dimensional stability scale. The relative development processes of the depth, length, and width of the jet scour were principally at the beginning of scour hole formation, while the development of the length and width lagged behind that of the scour length; here, $t/t_u = 0.1–0.2$, $L/$

L_u and B/B_u were approximately 0.70–0.80 or more, while the depths of all holes were more than 80% of the stable scour depth; as the scour continued to develop when $t/t_u = 0.3–0.4$, the scour depth substantially approached the final depth, i.e., $H/H_u > 0.90$; when $t/t_u > 0.5$, L/L_u and B/B_u progressively approached over 90% of the final scale of the scour hole. According to the comparative analysis of the hyperbolic tangent function curve and test data points, the relative time-domain processes of three-dimensional scales demonstrated a self-similar pattern for different water cushion depths T and scour Froude number Fr_d. The same formal curves were used to compare the relative lengths and widths of scour holes. During the development of scours and their morphological stabilization, the relative development of the hole morphology on both sides was generally consistent with the time-

FIGURE 6 | Prediction of the time-domain scour process: **(A)** H/H_u; **(B)** L/L_u and B/B_u.
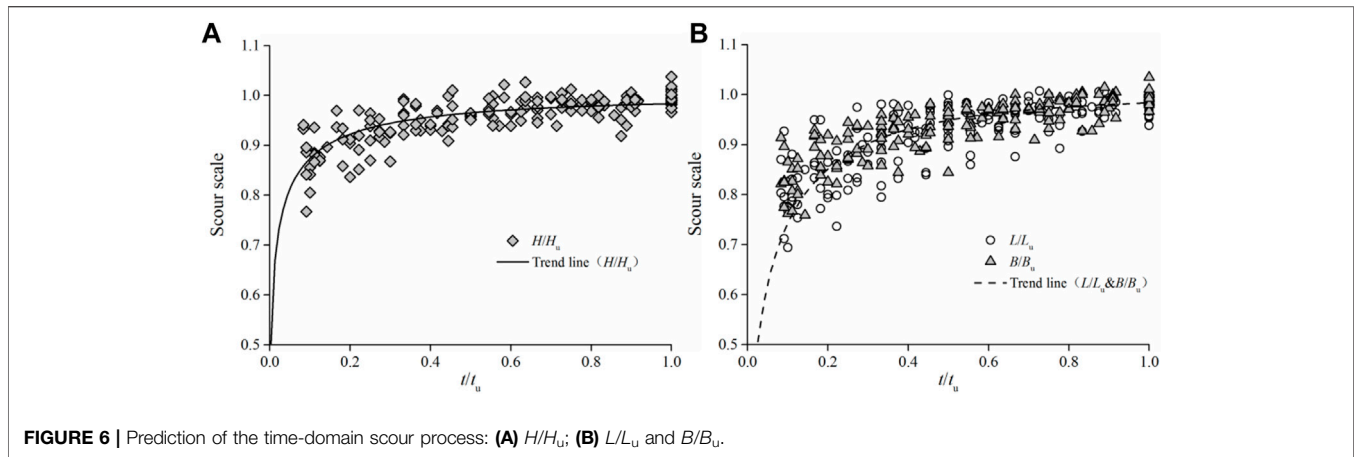
domain process. Analysis suggested that as the scour depth directly reflected the scouring capacity of the jet, it was principally influenced by the water transport capacity and the granular morphological stability during the stable formation in the two-dimensional directions of length and width, and the pattern adjustment could result in a longer period being required in the development of the scour when compared with the final stable morphology.

The relative scales, i.e., H/H_u, L/L_u, and B/B_u, among the time-domain process data at the three-dimensional scale of the scour were hyperbolic tangent to the relative time t/t_u, which is expressed as

$$H/H_u = \tanh\left[2.4\,(t/t_u)^{0.25}\right], \tag{1}$$

$$L/L_u = B/B_u = \tanh\left[2.4\,(t/t_u)^{0.40}\right]. \tag{2}$$

In such a case, the applicable conditions for water flow and the scour hole are as follows: $5.3 < Fr_d < 11.7$ and $14.0 < T/b < 19.0$. The comparison of the predicted time-domain processes on the relative morphological scour scale with test data is illustrated in **Figure 6**. The time-domain process curve substantially reflects the pattern of development of the jet scour on a three-dimensional scale to stable formation. Notably, these affecting factors such as hydrodynamic impact, sediment transport, and scour morphology adjustment at the initial stage of jet impingements resulted in the highly discrete fit analysis outcome at the early stage of scour formation. At $t/t_u = 0.2$, the H/H_u can reach 0.9, and the plane scales of the scour hole H/H_u and B/B_u increase to 0.7–0.8. As the developing period exceeds over a half of the entire process with $t/t_u > 0.5$, all scour hole scales get fully developed, and the relative error decreases as the hole gradually develops and stabilizes.
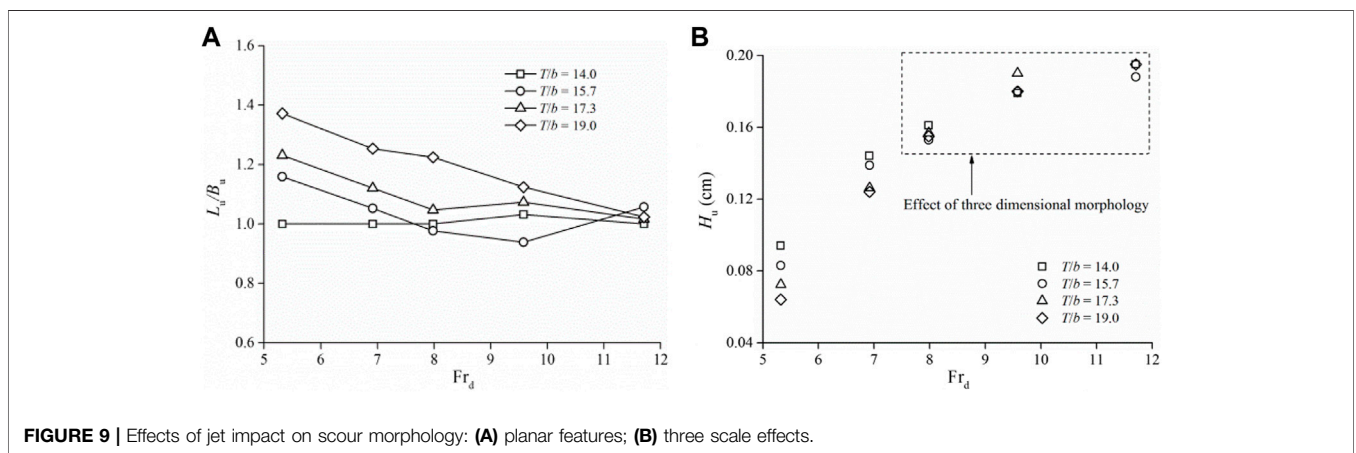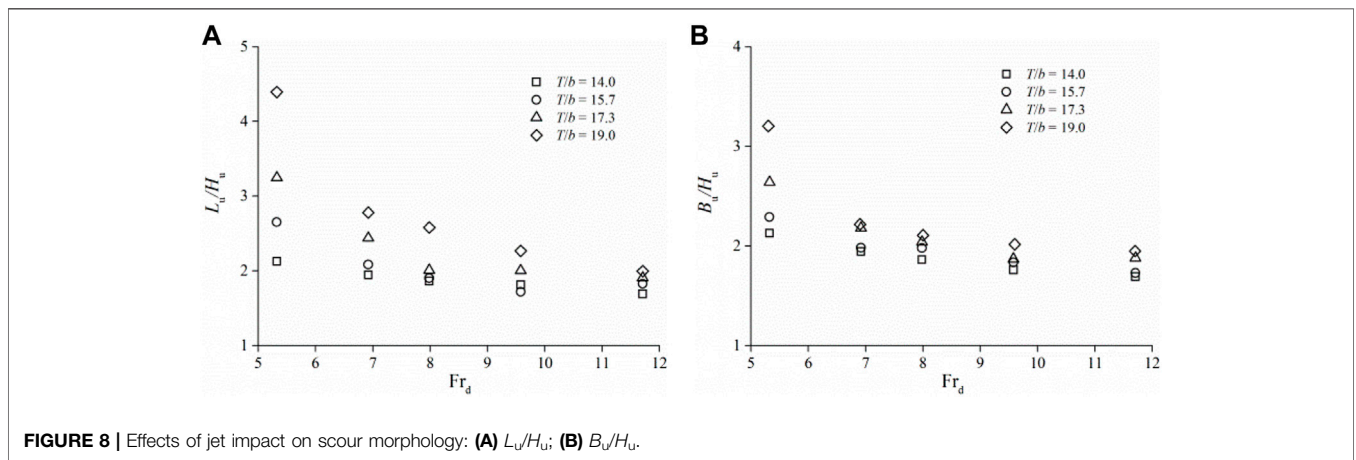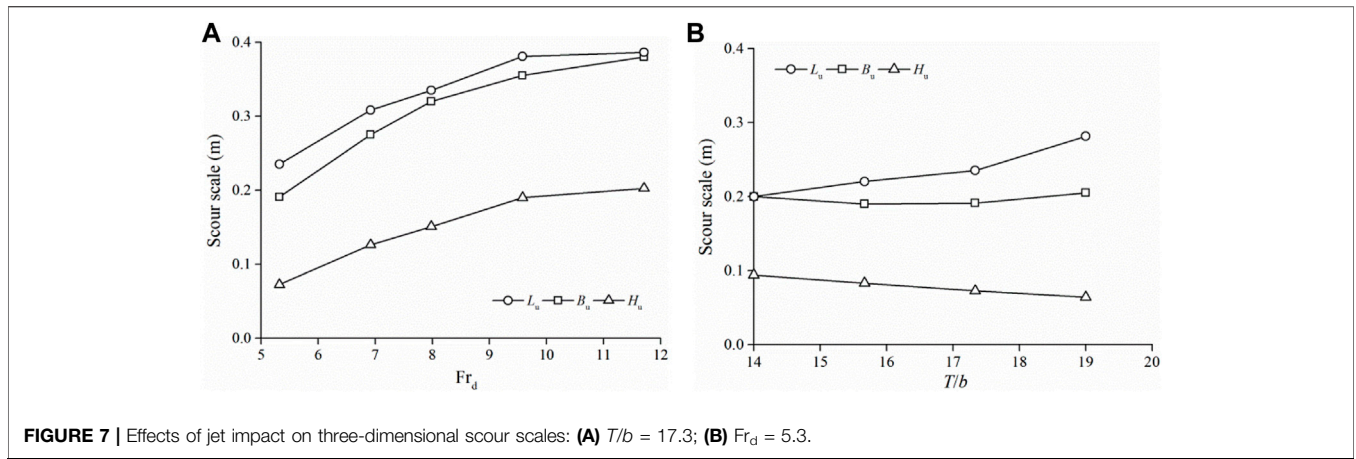
THREE-DIMENSIONAL MORPHOLOGY OF JET SCOUR

When the jet scour development became relatively stable, the test could identify the final three-dimensional scales of scour holes and their correlations by employing the depth H_u, length L_u, and

width B_u. **Figure 7** illustrates the effects of Fr_d and T/b conditions on H_u, L_u, and B_u scales. As Fr_d increased, the hydrodynamic scouring intensity progressively increased, as shown by a gradual increase in the scour scale in all directions. The scour depth decreased as the cushion depth increased and gradually increased with the scour length; when T/b increased from 14.0 to 19.0, the scour depth decreased from 0.094 to 0.063 m, while the length L_u increased from 0.200 to 0.282 m. In the meantime, the effect of cushion depth on the scour width was not obvious. It could, thus, be seen that the water cushion during the decrease in the hydraulic scour and the development of the scour depth were principally accompanied by an increase in the affected area of scour along the direction of water flow. The analyses suggest that the impact effects in the scour depth direction decreases after water flows through the water cushion energy dissipation area. The effect of the impingement jet flow on the scour hole depth is principally reflected in the fact that the particle transport of sediment in the direction of water flow dominates the extent of the wall attachment area.

The comparison of scale differences in the three-dimensional directions of the scour indicates that the hole scale in its length and width directions is significantly greater than that of the scour depth. With depth H_u as a reference, **Figure 8** illustrates the scaling relationship of the hole length and width relative to its depth and indicates its variation pattern with water flow conditions. Under weak scouring ($Fr_d = 5.3$) and a deeper water cushion ($T/b = 19.0$), the weaker hydrodynamic impact and enhanced energy dissipation of water cushion results in a decrease in the hole depth. Ultimately, the morphological length of the scour depth may reach more than four times the hole depth, and the hole width may reach more than 3-fold the depth. Moreover, as the hole depth continues to develop under strong scouring ($Fr_d > 9$–10) and a shallow water cushion ($T/b = 14.0$), the length-to-depth ratio L_u/H_u and the width-to-depth ratio B_u/H_u decreases progressively for the hole morphology, which shows a convergence of both to approx. 1.0–2.0.

With respect to the planar features of the jet scour, as shown in **Figures 9A**, a stronger hydraulic scouring capacity is obtained in the case of a shallow water cushion ($T/b = 14$). In terms of length and width, the morphology of the scour was substantially

FIGURE 7 | Effects of jet impact on three-dimensional scour scales: **(A)** T/b = 17.3; **(B)** Fr_d = 5.3.

FIGURE 8 | Effects of jet impact on scour morphology: **(A)** L_u/H_u; **(B)** B_u/H_u.

FIGURE 9 | Effects of jet impact on scour morphology: **(A)** planar features; **(B)** three scale effects.

constant. The effect of Fr_d on scour intensity was not significant, which behaved as though L_u/B_u was approximately 1.0. As the water cushion depth increased, the scour length varied more significantly than the scour width under low scouring intensity, which appeared as the length increased from 14.0 to 19.0 with T/b, while the length-to-width ratio increased to 1.40. As the

scouring intensity of water increased, L_u/B_u gradually decreased to 1.0, indicating that the scour development in the width direction became increasingly significant as the scouring capacity increased. The test result shows that this three-dimensional morphological feature of the scour hole had a certain effect on the scour depth prediction as the scour
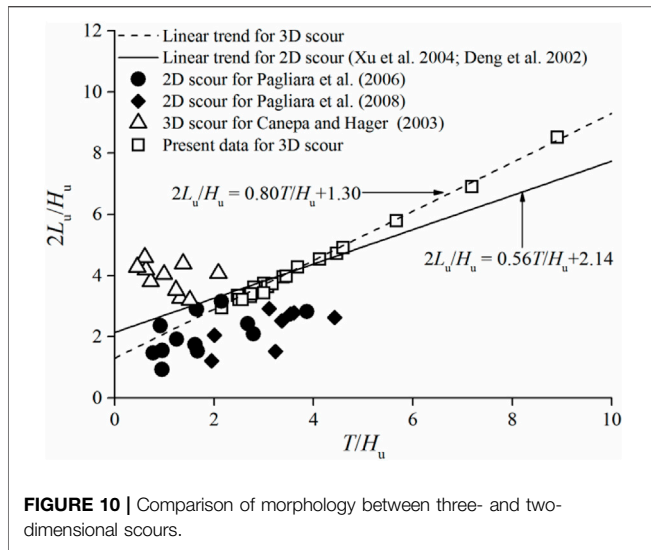
FIGURE 10 | Comparison of morphology between three- and two-dimensional scours.

developed and changed in the depth direction, along with the dramatic change in planimetric extent. As illustrated in **Figure 9B**, under low scour intensity (e.g., $Fr_d = 5.3$ or $Fr_d = 6.9$), the pattern change is more pronounced with increasing water cushion, leading to a progressively decreasing scour depth. However, with increasing scour intensity (when $Fr_d > 8.0$), the change in scour depth was not significant as the water cushion depth increased, indicating that the inhibiting effect of the change in the three-dimensional scales on the scour development was gradually manifested. At low jet flow velocity, the extent of the scour was small and the morphology was predominantly wide and shallow (L_u/H_u and B_u/H_u shown in **Figure 8** are significantly greater than 2.0), while the impact resistance in the direction of the scour depth was dominated by the energy dissipating effect of the water cushion. But as the jet flow velocity increased, the scale of the hole depth increased in and above the plane. Moreover, the broad and shallow morphology of the scour progressively diminished, which led to the gradual significant energy dissipation in the scour hole, which behaved as though the scour depth did not vary remarkably with water cushion

energy dissipation. From this point of view, the three-dimensional morphological characteristics of the scour had a substantial impact on the accurate determination of the final scour depth.

DEPTH COMPARISON BETWEEN TWO-DIMENSIONAL AND THREE-DIMENSIONAL SCOURS

The length-depth correlation was compared with the study of the two-dimensional scour in terms of three-dimensional scour morphology in the present test (**Figure 10**). Compared to the previous related experimental studies (Deng et al., 2002; Xu et al., 2004), the lengths of two-dimensional and three-dimensional scours increased linearly with the increasing water cushion depth. In the case of water cushion depth ($T/H_u > 5$), however, the three-dimensional scours are longer than two-dimensional scours. These scour morphology differences can also be observed from the other literature data, with different jet angles (Pagliara et al., 2006), impinging and submerged jet patterns (Canepa and Hager, 2003; Pagliara et al., 2008). In addition to the effects of the jet angle and impingement pattern on the jet velocity attenuation and the scour capacity, the scour morphology featured by three-dimensional scales is practically the same. The three-dimensional scour has a wider sediment range during the decrease in the scour depth by water cushion. The impact of water flow on the scour is principally manifested in the transportation of sediment in the direction of flow within the area of wall attachment, and this effect is even more pronounced in the case of a three-dimensional scour. Consequently, it is accompanied by the stable morphological feature of a gradually increasing length-to-width ratio in the longitudinal scour. The granular material size may contribute to the specific differences among the three-dimensional scours. The sand size for Canepa and Hager (2003) ranges from 0.010 to 0.019 m. The anti-flushing capacity for granular beds is stronger than the present condition. Thus, the scour development in the depth is weakened relatively, and the plane sand transportation is amplified, resulting in a larger L_u/H_u than that of the present measurement results.
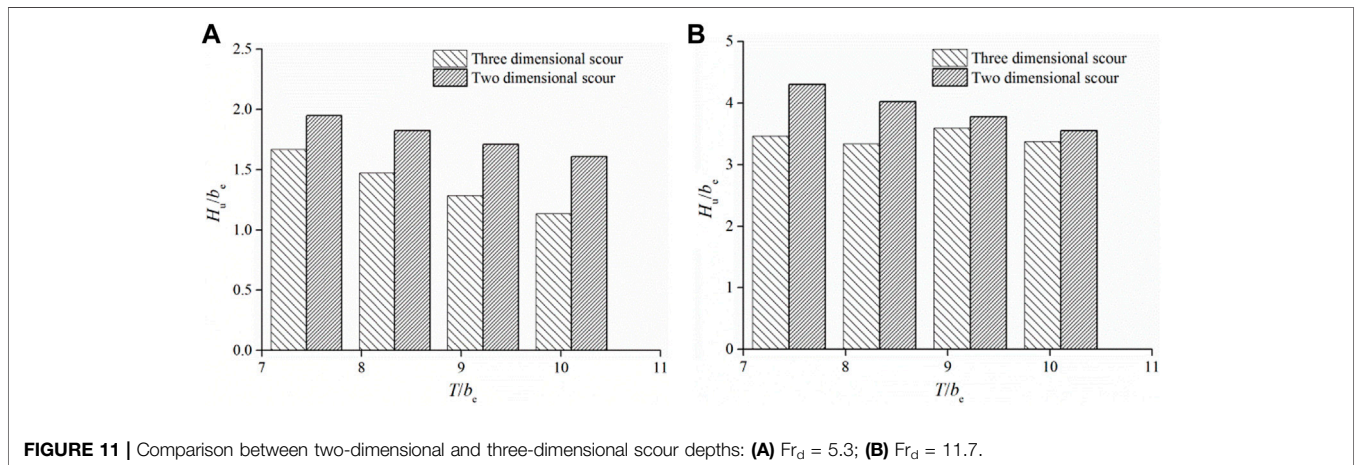

FIGURE 11 | Comparison between two-dimensional and three-dimensional scour depths: **(A)** $Fr_d = 5.3$; **(B)** $Fr_d = 11.7$.

Pagliara et al. (2006) systematically studied the prediction of two-dimensional scour depth by considering the effect of hydraulic conditions such as the jet impingement velocity (Fr_d), impact angle (θ), flow aeration (β), water cushion depth (T), and sediment particle size (d) on the scour depth, having proposed the empirical formula

$$H_u/b_e = f(\mathbf{Fr_d}) \cdot f(\theta) \cdot f(\beta) \cdot f(T) \cdot f(d). \quad (3)$$

With consideration of relevant scour hydraulic conditions in the present experimental study, the corresponding two-dimensional scour depth is calculated as follows:

$$H_u/b_e = 1.77 \cdot \mathbf{Fr_d} \cdot [0.12\ln(1/T) + 0.45] \cdot \sin(\theta + 22.5°), \quad (4)$$

where b_e represents the equivalent dimension of the jet flow; for rectangular sections, $b_e = (4bW/\pi)^{0.5}$. Under the conditions where $Fr_d = 5.3$ and $Fr_d = 11.7$, **Figure 11** indicates that the three-dimensional scour depth is significantly smaller than that of the two-dimensional scour depth. In conditions where $Fr_d = 5.3$ and $T/b_e = 10.1$, this difference amounts to approximately 30%. However, under high Fr_d, because of the extensive scour morphology, the change in the scour depth with water cushion depth under three-dimensional conditions is regularly different from that of the two-dimensional scour depth, which reduces the effect of water cushion depth on the reduction of the hole depth.

According to previous studies, the sediment transportation capacity during the scour generation process is correlated with the jet flow velocity (Stein et al., 1993; Jia et al., 2001). As the jet flow velocity decays, gradually impacting the solid surface of the scour hole, most sediment portions are carried out of the hole in the early scour generation period by the major roller in the axial jet zone (Si et al., 2018). As the jet velocity decreases, the sediment amount uplifted by the scour development reduces significantly. This is in accordance with the present research that the scour hole depth stops developing in the early stage. The secondary sediment movements include sediments moving and recirculating upstream, and other sediments entrained downstream but falling back to the scour hole. The main difference between the two- and three-dimensional scour depths indicates that in addition to the effect of jet velocity attenuation on the scour sediment, the three-dimensional scour may improve the scour hole sediment's remaining capacity in the scour. The data analysis results in a distinction between the two- and three-dimensional scour generations, providing a new insight into the three-dimensional scour evolution. All data relationships are obtained from the laboratory experiment measurements, which are limited to the test conditions. The present investigation is a potential step toward the understanding of the morphology and evolution of three-dimensional scours. Therefore, this work suits an appreciation of the temporal scour evolution of geological and hydraulic engineering applications.

CONCLUSION

Based on physical model tests, the present study measured the time-domain process of three-dimensional morphological scours generated by submerged jet impingements. The results suggested that the scour depth, length, and width varied dramatically at the initial stage of jet scour formation; the time-domain development processes in all directions of the scour exhibited self-similarity; the relative development rate of the scour length and width lagged behind that of the scour depth. For the scales in each direction under relatively stable scour development, as the jet velocity increased and the water cushion depth decreased, the scour scales increased in plane and elevation with increasing jet impingement intensity, while the energy dissipation in the scour hole gradually became substantial. The depth variation of the scour hole with the water cushion energy dissipation was insubstantial. The comparison with the two-dimensional scour scale suggested that the three-dimensional scour morphology had a certain inhibitory effect on the development of scour depth. The decrease in scour depth was accompanied by an increase in the scour length. The present experimental results offered an exploratory study on the three-dimensional morphological features of the jet scour formation, having to constitute the basis for more rational analysis and evaluation of hydraulic operations in water conservancy projects.

DATA AVAILABILITY STATEMENT

The original contributions presented in the study are included in the article/supplementary material; further inquiries can be directed to the corresponding author.

AUTHOR CONTRIBUTIONS

K-LC and WW conducted the experimental tests and data analysis. The main text was written by WW and K-LC. Jun Deng provided detailed guidance about the hydraulic model tests.

FUNDING

REFERENCES

Adduce, C., and La Rocca, M. (2006). Local Scouring Due to Turbulent Water Jets Downstream of a Trapezoidal Drop: Laboratory Experiments and Stability Analysis. *Water Resour. Res.* 42 (2), W02405. doi:10.1029/2005WR004139

Beltaos, S., and Rajaratnam, N. (1973). Plane Turbulent Impinging Jets. *J. Hydraulic Res.* 11, 29–59. doi:10.1080/00221687309499789

Ben Meftah, M., and Mossa, M. (2006). Scour Holes Downstream of Bed Sills in Low-Gradient Channels. *J. Hydraulic Res.* 44, 497–509. doi:10.1080/00221686.2006.9521701

Bombardelli, F. A., Palermo, M., and Pagliara, S. (2018). Temporal Evolution of Jet Induced Scour Depth in Cohesionless Granular Beds and the

Phenomenological Theory of Turbulence. *Phys. Fluids* 30, 085109. doi:10.1063/1.5041800

Boniforti, M. A., Guercio, R., and Magini, R. (2015). Effects of Submerged Sheet Pile Vanes on Mobile River Beds. *J. Zhejiang Univ. Sci. A* 16, 182–193. doi:10.1631/JZUS.A1400336

Bormann, N. E., and Julien, P. Y. (1991). Scour Downstream of Grade-Control Structures. *J. Hydraulic Eng.* 117, 579–594. doi:10.1061/(asce)0733-9429(1991)117:5(579)

Canepa, S., and Hager, W. H. (2003). Effect of Jet Air Content on Plunge Pool Scour. *J. Hydraul. Eng.* 128, 358–365. doi:10.1061/(asce)0733-9429(2003)129:5(358)

Deng, J., Xu, W. L., Qu, J. X., and Yang, Y. Q. (2002). Influence of Aeration on Scouring. *Shuili Xuebao* 10, 8–13. (in Chinese). doi:10.3321/j.issn:0559-9350.2002.10.002

Dey, S., and Barbhuiya, A. K. (2005). Time Variation of Scour at Abutments. *J. Hydraul. Eng.* 131, 11–23. doi:10.1061/(asce)0733-9429(2005)131:1(11)

Dey, S., and Sarkar, A. (2008). Characteristics of Submerged Jets in Evolving Scour Hole Downstream of an Apron. *J. Eng. Mech.* 134 (11), 927–936. doi:10.1061/(asce)0733-9399(2008)134:11(927)

Gaudio, R., and Marion, A. (2003). Time Evolution of Scouring Downstream of Bed Sills. *J. Hydraulic Res.* 41, 271–284. doi:10.1080/00221680309499972

Guan, D., Melville, B. W., and Friedrich, H. (2014). Flow Patterns and Turbulence Structures in a Scour Hole Downstream of a Submerged Weir. *J. Hydraul. Eng.* 140 (1), 68–76. doi:10.1061/(ASCE)HY.1943-7900.0000803

Hill, D. F., and Younkin, B. D. (2006). PIV Measurements of Flow in and Around Scour Holes. *Exp. Fluids* 41 (2), 295–307. doi:10.1007/s00348-006-0156-3

Jia, Y., Kitamura, T., and Wang, S. S. Y. (2001). Simulation of Scour Process in Plunging Pool of Loose Bed-Material. *J. Hydraul. Eng.* 127 (3), 219–229. doi:10.1061/(ASCE)0733-9429(2001)127:3(219)

Lenzi, M. A., Marion, A., Comiti, F., and Gaudio, R. (2002). Local Scouring in Low and High Gradient Streams at Bed Sills. *J. Hydraulic Res.* 40, 731–739. doi:10.1080/00221680209499919

Li, J.-n., Zhang, J.-m., and Peng, Y. (2017). Characterization of the Mean Velocity of a Circular Jet in a Bounded Basin. *J. Zhejiang Univ. Sci. A* 18, 807–818. doi:10.1631/jzus.A1600761

Liu, P., Gao, J., and Li, Y. (1998). Experimental Investigation of Submerged Impinging Jets in a Plunge Pool Downstream of Large Dams. *Sci. China Ser. E-Technol. Sci.* 41 (4), 357–365. doi:10.1007/BF02917007

Liu, Q.-s., Tang, H.-w., Wang, H., and Xiao, J.-f. (2018). Critical Velocities for Local Scour Around Twin Piers in Tandem. *J. Hydrodyn.* 30, 1165–1173. doi:10.1007/s42241-018-0122-6

Mason, P. J. (1989). Effects of Air Entrainment on Plunge Pool Scour. *J. Hydraulic Eng.* 115, 385–399. doi:10.1061/(ASCE)0733-9429(1989)115:3(385)

Pagliara, S., Hager, W. H., and Minor, H.-E. (2006). Hydraulics of Plane Plunge Pool Scour. *J. Hydraul. Eng.* 132, 450–461. doi:10.1061/(ASCE)0733-9429(2006)132:5(450)

Pagliara, S., Hager, W. H., and Unger, J. (2008a). Temporal Evolution of Plunge Pool Scour. *J. Hydraul. Eng.* 134, 1630–1638. doi:10.1061/(ASCE)0733-9429(2008)134:11(1630)

Pagliara, S., Mahmoudi Kurdistani, S., Palermo, M., and Simoni, D. (2016). Scour Due to Rock Sills in Straight and Curved Horizontal Channels. *J. Hydro-environment Res.* 10, 12–20. doi:10.1016/j.jher.2015.07.002

Pagliara, S., and Palermo, M. (2008b). Plane Plunge Pool Scour with Protection Structures. *J. Hydro-environment Res.* 2, 182–191. doi:10.1016/j.jher.2008.06.002

Pagliara, S., Palermo, M., and Roy, D. (2020). Experimental Investigation of Erosion Processes Downstream of Block Ramps in Mild Curved Channels. *Environ. Fluid Mech.* 20, 339–356. doi:10.1007/s10652-019-09681-1

Pagliara, S., and Palermo, M. (2017). Scour Process Caused by Multiple Subvertical Non-crossing Jets. *Water Sci. Eng.* 10, 17–24. doi:10.1016/j.wse.2017.03.010

Qian, S.-t., Zhang, Y., Xu, H., Wang, X.-s., Feng, J.-g., and Li, Z.-x. (2021). Effects of Surface Roughness on Overflow Discharge of Embankment Weirs. *J. Hydrodyn.* 33, 773–781. doi:10.1007/s42241-021-0068-y

Si, J.-H., Lim, S.-Y., and Wang, X.-K. (2018). Flow Structures in Evolving Scour Holes Caused by a Plunging Jet Downstream of a Weir. *J. Hydraul. Eng.* 144 (6), 04018018. doi:10.1061/(ASCE)HY.1943-7900.0001452

Stein, O. R., Julien, P. Y., and Alonso, C. V. (1993). Mechanics of Jet Scour Downstream of a Headcut. *J. Hydraulic Res.* 31 (6), 723–738. doi:10.1080/00221689309498814

Wang, L., Melville, B. W., Guan, D., and Whittaker, C. N. (2018). Local Scour at Downstream Sloped Submerged Weirs. *J. Hydraul. Eng.* 144, 04018044. doi:10.1061/(ASCE)HY.1943-7900.0001492

Wang, L., Melville, B. W., Whittaker, C. N., and Guan, D. (2020). Temporal Evolution of Clear-Water Scour Depth at Submerged Weirs. *J. Hydraul. Eng.* 146, 06020001. doi:10.1061/(ASCE)HY.1943-7900.0001712

Xu, W., Deng, J., Qu, J., Liu, S., and Wang, W. (2004). Experimental Investigation on Influence of Aeration on Plane Jet Scour. *J. Hydraul. Eng.* 130, 160–164. doi:10.1061/(ASCE)0733-9429(2004)130:2(160)

Yao, L., and Wu, J.-h. (2020). Local Scour by Multiple Slit-type Energy Dissipaters. *J. Hydrodyn.* 32, 1221–1224. doi:10.1007/s42241-020-0068-3